Network Mechanism for Burst Generation

Mikhail V. Ivanchenko,[1,2] Grigory V. Osipov,[1,2] Vladimir D. Shalfeev,[1] and Jürgen Kurths[2]

[1]*Department of Radiophysics, Nizhny Novgorod University, 23, Gagarin Avenue, 603950 Nizhny Novgorod, Russia*

[2]*Institute of Physics, University Potsdam, 10, Am Neuen Palais, D-14415, Potsdam, Germany*

(Received 10 January 2006; published 5 March 2007)

We report on the mechanism of burst generation by populations of intrinsically spiking neurons, when a certain threshold in coupling strength is exceeded. These ensembles synchronize at relatively low coupling strength and lose synchronization at stronger coupling via spatiotemporal intermittency. The latter transition triggers fast repetitive spiking, which results in synchronized bursting. We present evidence that this mechanism is generic for various network topologies from regular to small-world and scale-free ones, different types of coupling and neuronal model.

DOI: 10.1103/PhysRevLett.98.108101 PACS numbers: 87.19.La, 05.45.Xt

Bursting is a fundamental regime of neuronal behavior, exhibiting trains of spikes of the action potential mediated by periods of silence [1]. In some cases its functional importance, like coordinating movements by antiphase synchronized bursts from central pattern generators [2], is pretty well understood. In other cases, like synchronous high- (>300 Hz) or low-frequency (<300 Hz) bursting in cortical areas of the behaving or sleeping animal [3], it is less apparent, leaving place for hypothesizing about its role in learning, cognition, motivation, movement control, increasing reliability of cortical synapses [4,5] or provoking neural disorders [6].

Remarkably, the problem of the origin of bursting in neural ensembles appears to be even more challenging than its synchronization alone, for which (in case of coupled intrinsically bursting neurons) a well-developed theory [7] is often applied. Quite on the contrary, there is a constantly increasing experimental and theoretical evidence of versatile network mechanisms of burst generation in ensembles of neurons, which are not intrinsically bursting.

Reciprocal asymmetric inhibition can launch sequential bursting or so-called winnerless competition dynamics [8], which has been proposed to explain the hunting behavior of the marine mollusk *Clione* [9]. Another network mechanism is suggested by experiments with developing networks of cultured cortical neurons and biological and numerical studies of deafferented cortical slabs [10]. It comprises initiation of the first spike in an occasional cell by randomlike miniature excitatory potentials and the further development and termination of the overall bursting due to excitatory and inhibitory synapses.

There are strong indications that deterministic noninhibitory networks are able of generating bursts too. Several modeling studies reported the origin of bursting in spiking neural networks under weak electrical coupling, while for stronger coupling the synchronized spiking regime would be observed [11]. In some discrepancy with these results, biological experiments and their detailed computational reproduction have demonstrated synchronous high-frequency spiking at moderate electrical coupling between two midbrain dopamine neurons [12]. The transition to bursting occurred at stronger coupling via generation of the slow time-scale (STS) oscillations. At the same time, intrinsic low-frequency spiking would not generate high-frequency repetitive spikes and remained stable at large coupling, in agreement with [11]. The current study was inspired by a recent finding, showing that the latter pathway can be realized in large networks of electrically coupled neuronal-type models [13].

In this Letter we introduce a network mechanism of generation of synchronized bursting by intrinsically spiking neurons without inhibition. We demonstrate that spikes creating effective afterdepolarizations (ADPs) in adjacent neurons cause instability of the regime of synchronous spiking, as the strength of electrical or excitatory coupling is increased. This instability excites occasional fast repetitive spiking, which constitute irregular bursting. At stronger coupling bursts get regularized and synchronized. In chain ensembles the instability manifests the properties of the spatiotemporal intermittency and size-independent threshold. Simulations of scale-free and small-world topologies as well as representing a neuron by a Hodgkin-Huxley type model give evidence of ubiquity of this phenomenon in complex neuronal networks.

We consider networks of nonidentical neuronal model maps, proposed in [14], basing our choice on its computational efficiency:

$$\begin{cases} x_j^{k+1} = f(x_j^k, x_j^{k-1}, y_j^k) + \varepsilon \sum_i G_{j,i}^k / K_i, \\ y_j^{k+1} = y_j^k + \mu(-x_j^k - 1 + \varsigma_j + \varepsilon \sum_i G_{j,i}^k / K_i), \end{cases} \tag{1}$$

$$f(x, \tilde{x}, y) = \begin{cases} \alpha/(1-x) + y, & \text{if } x \le 0, \\ \alpha + y, & \text{if } 0 < x < \alpha + y \quad \text{and } \tilde{x} \le 0, \\ -1, & \text{if } x \ge \alpha + y \quad \text{or } \tilde{x} > 0 \end{cases} \tag{2}$$

where x_j and y_j are the fast and slow variables, respectively, $j = \overline{1, N}$. In all simulations we use $\mu = 10^{-3}$, $\alpha = 3.5$, $\varsigma_i \in [0.15, 0.16]$ (a uniform random distribution) that provides chaotic spiking in an isolated map; ε is the coupling strength, K_i is the number of entries in the ith neuron. The sum is taken over all neighbors of a neuron in the network; all connections are reciprocal. The coupling function corresponds either to electrical $G^k_{j,i} = x^k_i - x^k_j$, or excitatory coupling $G^k_{j,i} = (x_{\rm rp} - x_j)\chi(x_i)$, here the reversal potential $x_{\rm rp} = 1$, $\chi(x) = 1$ if $x > 0$, and $\chi(x) = 0$ otherwise, the fast synapse (the synaptic time equals to unity) is assumed.

Synchronization-desynchronization transitions are decisive for the dynamics of this neural ensemble, thus we analyze it in terms of chaotic phase synchronization (CPS) [15]. For each neuron we calculate the average frequencies of spiking ω_j and slow time-scale oscillations Ω_j. Definition of the spiking frequency assumes that each spike contributes a 2π growth of the phase of spiking. A 2π increase of the phase of STS oscillations occurs only when the interval of silence between two spikes exceeds 80 iterations. Note, that while neurons generate STS chaotic spiking (like for $\varepsilon = 0$), both definitions are equivalent. If fast repetitive spikes form trains of bursts, Ω_j will characterize the bursting frequency and ω_j will characterize the average spiking frequency. This technique allows for a correct separation of the fast time-scale (FTS) and STS.

Now we summarize the regimes that occur for different coupling strengths ε in a regular chain of electrically coupled neurons [13]. At low coupling neuronal firings are unsynchronized [Fig. 1(a)], at moderate coupling they get synchronized [Fig. 1(b)]. As we increase ε, the CPS regime becomes unstable and neurons start firing fast repetitive spikes occasionally thus forming irregular bursts [Fig. 1(c)]. Further increase of ε results in regular synchronized bursts with a fractal-like spatiotemporal structure of spikes [Fig. 1(d)] [16].

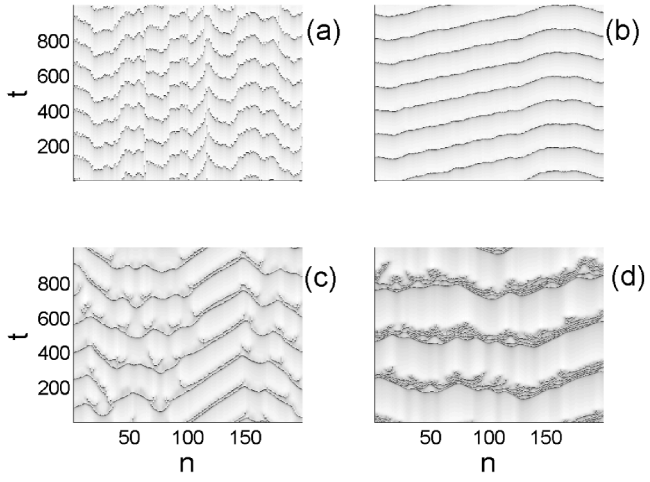

FIG. 1. Space-time plots illustrate different regimes that occur in the chain (1). x_j values are represented by gray scale, white corresponds to minimal values, black to maximal ones. Shown are (a) unsynchronized spiking, $\varepsilon = 0.01$, (b) synchronized spiking, $\varepsilon = 0.05$, (c) desynchronized state and irregular bursts: synchronization is occasionally broken by fast repetitive spikes, $\varepsilon = 0.1$, (d) synchronized bursts with a fractal-like spatiotemporal structure of spikes, $\varepsilon = 0.2$.

To quantify these transitions we have computed the variances of the STS and spiking time-scale oscillations frequencies vs the strength of the electrical coupling for the chain lengths $N = 200$, 400, 800 (Fig. 2). We find two threshold coupling strengths: $\varepsilon_1 \approx 0.035$, $\varepsilon_2 \approx 0.07$, and quite a smooth transition near $\varepsilon_3 \approx 0.15$. No substantial size dependence of these thresholds is observed in large networks. In small networks ($N < 50$) the instability of spiking CPS becomes depressed and ε_2 rapidly increases with decreasing N. The thresholds define four intervals: (i) for $\varepsilon \in [0, \varepsilon_1]$ oscillations on the single existing time-scale—the slow one—are unsynchronized, (ii) for $\varepsilon \in [\varepsilon_1, \varepsilon_2]$ oscillations on the STS are synchronized, (iii) for $\varepsilon \in [\varepsilon_2, \varepsilon_3]$ oscillations on the second time-scale—the fast one—are generated and form irregular bursts, (iv) and for large coupling $\varepsilon > \varepsilon_3$ regular STS oscillations form synchronized bursting, oscillations on the FTS remain unsynchronized.

The transition to CPS at ε_1 is a conventional way how arrays of nonidentical oscillators behave [7]. The process of burst regularization and synchronization has also been described [17]. The problem to be in focus is the mechanism of burst generation, which comprises the instability of CPS at ε_2 and the generation of the FTS by repetitive spikes and irregular bursting further on.

To uncover its nature, we record the interspike intervals T_s in every neuron and plot their evolution for different coupling strengths on one figure (Fig. 3). For $\varepsilon < \varepsilon_2$ we observe that chaotic spikes construct only the STS ($T_s > 100$), be it unsynchronized [Fig. 3(a)] or synchronized [Fig. 3(b)] dynamics. Note that in the synchronization regime the relative spike timing in neurons is locked but

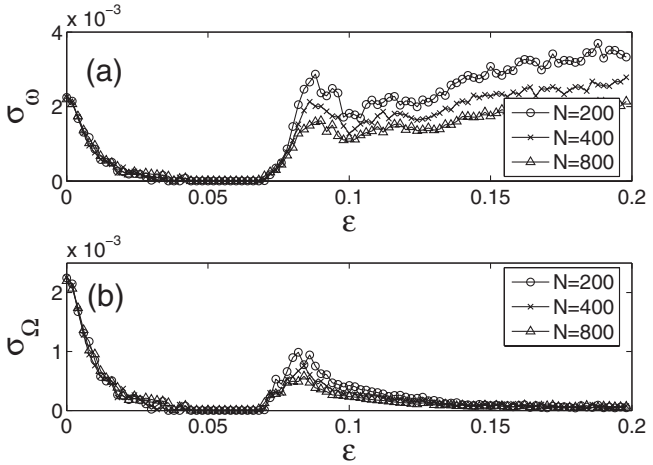

FIG. 2. Variances of spiking and slow time-scale (STS) frequencies ω_j and Ω_j over the chain (1) vs coupling strength ε for different chain sizes N.

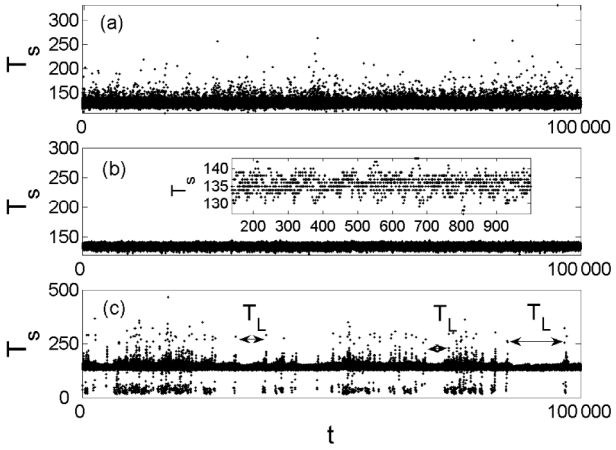

FIG. 3. Evolution of interspike intervals for (a) $\varepsilon = 0.01$, (b) $\varepsilon = 0.05$, (c) $\varepsilon = 0.073$. In (c) we denote several windows of CPS T_L.

not tightly fixed, typically of genuine CPS [see the inset in Fig. 3(b)]. T_s sequences [Fig. 3(c)] demonstrate the intermittent nature of the developing instability. The time intervals, during which fast repetitive spikes are generated, are interrupted by windows of synchronized STS spiking [Fig. 3(c)]. The closer ε is to ε_2, the larger become windows of CPS. In Figs. 4(a) and 4(c) we show statistical properties of interspike intervals T_s and time durations of windows of CPS T_L, respectively. Remarkably, the probability distributions of T_L demonstrate a power-law dependence over five decades in a finite interval of the coupling strength with ε-dependent exponents.

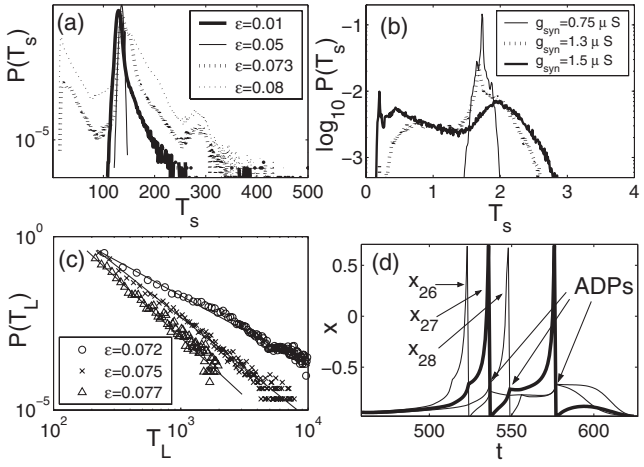

FIG. 4. Probability distributions of interspike intervals $P(T_s)$ in chains of (a) electrically coupled Rulkov's model neurons ($N = 200$) and (b) excitatory coupled Hodgkin-Huxley type neurons ($N = 50$). For Rulkov's model neurons follow (c) duration of stable CPS windows $P(T_L)$ for different values of the coupling strength (solid lines are guides for an eye) and (d) dynamics of fast variables x_j in three neighbored neurons [generation of ADPs and a fast repetitive spike in the 27th neuron (bold line) by the 28th].

The instability is triggered when a spike in an adjacent neuron creates or enhance an ADP in a just fired neuron [afterdepolarizations indicated by arrows in Fig. 4(d)]. Should the coupling be strong enough the ADP transforms into a fast repetitive spike (note the second spike in the 27th neuron in Fig. 4(d)]. The presence of the small parameter μ allows us to separate dynamics of autonomous maps (1), $\varepsilon = 0$, into slow and fast motions [14]. Applying the standard analysis we can approximate the curve for slow motions by $y = x + \alpha/(x-1)$, its stable and unstable parts being $\{W^{s,u}\colon x^{s,u} = (1 + y \mp \sqrt{(1-y)^2 - 4\alpha})/2\}$. The slow motion along W^s corresponds to periods of silence, W^u separates fast trajectories converging to W^s and those corresponding to spikes. Therefore, W^u gives a threshold to be overcome by an ADP for it to result in a repetitive spike, an estimation reads $x^u(y) - x^s(y) = \sqrt{(1-y)^2 - 4\alpha}$. Note, that this threshold increases with decrease of y (y is essentially negative). Termination of network generated bursts can be explained too. During sequential spiking y substantially decreases, as the trajectory spends most of the time above the nullcline $\{x^k = -1 + \varsigma\colon y^{k+1} = y^k\}$ (1). Thus, after several spikes, a neighbor-generated ADP cannot exceed grown threshold and the burst ends.

Electrical coupling synchronizes interacting neurons until the faster neuron fires (excitatory coupling leaves this stage neutral). Its firing is also a synchronizing event, as it pushes the slower oscillator up [note a depolarization of the 27th neuron just after a spike in the 26th at time $t \approx 530$ in Fig. 4(d)]. On the opposite, firing of the slower neuron desynchronizes them, as it pushes the faster one up towards the next firing, creating an effective ADP [in the 27th neuron at $t \approx 550$, caused by a spike in the 28th neuron, see Fig. 4(d)]. Varying ε we change the balance between synchronization and desynchronization and observe the instability of synchronization when short desynchronizing intervals prevail.

To test for this mechanism on the most realistic class of model neurons, we chose one of the Hodgkin-Huxley–type models (for description and original parameters see [18], we modified $g_{\text{Na-}V} = 0.09$, $g_B = 0.06$ that ensures intrinsic spiking). The simulations were carried out in chains of *electrically* or *excitatory* coupled neurons, the coupling term (synaptic current) being $I^{\text{syn}} = g_{\text{syn}}(V_{\text{pre}} - V_{\text{post}})$ in case of electrical coupling and $I^{\text{syn}} = g_{\text{syn}} r(t)(E_{\text{syn}} - V_{\text{post}})$ in case of excitatory. Here V_{pre}, V_{post} are pre- and postsynaptic potentials, $E_{\text{syn}} = 0$ is the reversal potential, $\dot{r} = \alpha_s A(1-r) - \beta_s r$, $\alpha_s = 500\ \text{s}^{-1}$, $\beta_s = 20\ \text{s}^{-1}$, $A = 0.5$ during 2 ms after a spike and $A = 0.0$ otherwise [19]. A depolarizing dc current $I \in [0; 0.02\ \text{nA}]$ (taken randomly) was assigned. We observed similar transitions as above, the threshold values being $g_{\text{syn},1} \approx 0.2\ \mu\text{S}$, $g_{\text{syn},2} \approx 0.4\ \mu\text{S}$, $g_{\text{syn},3} \approx 1.3\ \mu\text{S}$ for electrical coupling and $g_{\text{syn},1} \approx 0.6\ \mu\text{S}$, $g_{\text{syn},2} \approx 0.8\ \mu\text{S}$, $g_{\text{syn},3} \approx 2.5\ \mu\text{S}$ for excitatory. Distributions of the interspike intervals $P(T_s)$ near the

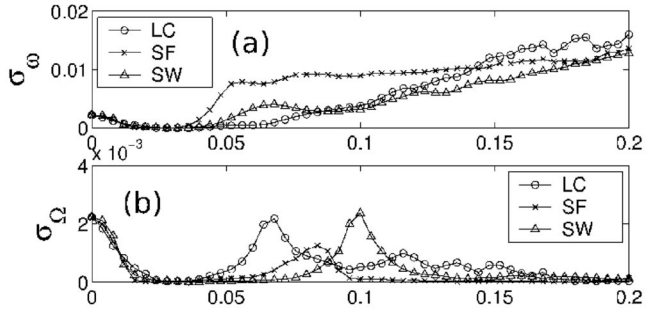

FIG. 5. Variances of (a) spiking and (b) STS frequencies ω_j and Ω_j vs excitatory coupling strength for local coupling (LC), scale-free (SF), and small-world (SW) network topologies ($N = 200$, averages over 100 realizations shown).

instability threshold [Fig. 4(b)] are qualitatively the same as in case of Rulkov's model neuron [Fig. 4(a)].

To demonstrate persistence of the studied mechanism in complex networks we turn back to the Rulkov's model and implement scale-free and small-world topologies [20] and assume excitatory coupling. The scale-free network we simulate is characterized by the node degree K distribution $P(K) \propto K^{-\gamma}$, $\gamma = 2.2$ (with regard to the recent experimental study of connectivity of functional brain networks [21]), and the mean $\langle K \rangle \approx 4.2$. The small-world network has on the average 10 links per neuron and the probability of rewiring a short-range regular link is $p = 0.1$. The results of the simulations [Figs. 5(a) and 5(b)] demonstrate the same scenario of the onset of bursting via instability of synchronized chaotic spiking. This similarity becomes quite natural, as one takes into account that fast repetitive spiking is the result of neighbor-to-neighbor interactions, as discussed above.

In summary, we have demonstrated a deterministic network mechanism of burst generation by intrinsically spiking neurons without inhibition. The increased electrical or excitatory coupling created and enhanced afterdepolarizations in neighbor neurons thus leading to the instability of synchronous spiking. Exceeding a certain size-independent threshold of instability launched occasional fast repetitive spikes and the onset of irregular bursting in the network, to be regularized and synchronized at stronger coupling. In chain ensembles this instability was characterized as the spatiotemporal intermittency. This mechanism was shown to persist in complex networks, under electrical or excitatory coupling and within a Hodgkin-Huxley type model. Beside an apparent impact on the theory of generation and synchronization of oscillations on multiple time-scales, these findings may directly apply to neurobiological systems, revealing one of the possible mechanisms for burst origin. Another prediction is that bursting should appear more often than spiking in large-scale neuronal networks. And we strongly expect the reported mechanism to be observed in biological experiments.

The authors thank M. I. Rabinovich and the referees for highly valuable remarks. M. I. acknowledges financial support of INTAS YS 04-83-2816; G. O. acknowledges RFBR Nos. 05-02-90567, 05-02-19815, 06-02-16596 and Gastproffessor des Interdisziplinären Zentrum für Kognitive Studien für Komplexer Systeme; and J. K. that of the International Promotionskolleg Cognitive Neuroscience and BIOSIM.

[1] X.-J. Wang and J. Rinzel, in *Handbook of Brain Theory and Neural Networks*, edited by M. A. Arbib (MIT Press, Cambridge, MA, 1995).
[2] E. Marder and R. L. Calabrese, Physiol. Rev. **76**, 687 (1996); S. Grillner, Nat. Rev. Neurosci. **4**, 573 (2003).
[3] M. Steriade, D. A. McCormick, and T. J. Sejnowski, Science **262**, 679 (1993).
[4] A. K. Engel, P. Fries, and W. Singer, Nat. Rev. Neurosci. **2**, 704 (2001); A. Schnitzler and J. Gross, Nat. Rev. Neurosci. **6**, 285 (2005); M. I. Rabinovich *et al.*, Rev. Mod. Phys. **78**, 1213 (2006).
[5] J. E. Lisman, Trends Neurosci. **20**, 38 (1997).
[6] W. D. Hutchison *et al.*, J. Neurosci. **24**, 9240 (2004); I. Timofeev and M. Steriade, Neuroscience **123**, 299 (2004); P. Tass *et al.*, Phys. Rev. Lett. **81**, 3291 (1998).
[7] A. S. Pikovsky, M. G. Rosenblum, and J. Kurths, *Synchronization: A Universal Concept in Nonlinear Sciences* (Cambridge University Press, Cambridge, U.K., 2001); S. Boccaletti *et al.*, Phys. Rep. **366**, 1 (2002).
[8] M. I. Rabinovich *et al.*, Phys. Rev. Lett. **87**, 068102 (2001).
[9] R. Levi *et al.*, J. Neurophysiol. **91**, 336 (2004); R. Levi *et al.*, J. Neurosci. **25**, 9807 (2005).
[10] E. Maeda, H. P. C. Robinson, and A. Kawana, J. Neurosci. **15**, 6834 (1995); I. Timofeev *et al.*, Cereb. Cortex **10**, 1185 (2000).
[11] A. Sherman and J. Rinzel, Proc. Natl. Acad. Sci. U.S.A. **89**, 2471 (1992); C. C. Chow and N. Kopell, Neural Comput. **12**, 1643 (2000).
[12] A. O. Komendantov and C. C. Canavier, J. Neurophysiol. **87**, 1526 (2002).
[13] G. V. Osipov *et al.*, Phys. Rev. E **71**, 056209 (2005).
[14] N. F. Rulkov, Phys. Rev. E **65**, 041922 (2002); N. F. Rulkov, I. Timofeev, and M. Bazhenov, J. Comput. Neurosci. **17**, 203 (2004).
[15] M. G. Rosenblum, A. S. Pikovsky, and J. Kurths, Phys. Rev. Lett. **76**, 1804 (1996).
[16] Note, that self-sustained fractal-like patterns of spikes may arise in result of the instability of travelling waves in excitable systems too, see V. B. Kazantsev *et al.*, Phys. Rev. E **68**, 017201 (2003), and references therein.
[17] N. F. Rulkov, Phys. Rev. Lett. **86**, 183 (2001).
[18] A. O. Komendantov and N. I. Kononenko, J. Theor. Biol. **183**, 219 (1996).
[19] A. Destexhe, Z. F. Mainen, and T. J. Sejnowski, J. Comput. Neurosci. **1**, 195 (1994).
[20] S. H. Strogatz, Nature (London) **410**, 268 (2001); R. Albert and A. L. Barabási, Rev. Mod. Phys. **74**, 47 (2002).
[21] V. M. Eguiluz *et al.*, Phys. Rev. Lett. **94**, 018102 (2005).